Replicating the facilitatory effects of transcranial random noise stimulation on motion processing: A registered report

Mica B. Carroll[1*], Grace Edwards[1*], Chris I. Baker[1]

[1]Laboratory of Brain and Cognition, National Institute of Mental Health, Bethesda, MD, USA

*Equally contributed

Corresponding author

Grace Edwards: grace.edwards@nih.gov

New address: The National Institutes of Health, NIMH, Laboratory of Brain and Cognition, 10 Center Drive, Room 4C104, Bethesda MD 20892-1366

Keywords:

tRNS; hMT+; facilitation; maximum likelihood procedure; motion coherence; vision

Abstract

Non-invasive brain stimulation (NIBS) techniques have the potential to demonstrate the causal impact of targeted brain regions on specific behaviors, and to regulate or facilitate behavior in clinical applications. Transcranial random noise stimulation (tRNS) is one form of transcranial electric stimulation (tES) in which an alternating current is passed between electrodes at random frequencies. High-frequency tRNS (hf-tRNS) is thought to enhance excitability and has been reported to have facilitatory effects on behavior in healthy and clinical populations. Due to the potential application of tRNS, clear demonstrations of the efficacy and replicability of stimulation are critical. Here, we propose to replicate the facilitatory effect of hf-tRNS over the human middle temporal complex (hMT+) on contralateral motion processing, initially demonstrated by Ghin et al. (2018). The improvement in performance was specific to global motion processing in the visual field contralateral to stimulation. The motivation to replicate this effect is reinforced by the well-supported hypothesis that hMT+ is critical for contralateral global motion processing. We hypothesize that we will replicate the facilitatory effect of hf-tRNS to hMT+ on contralateral global motion processing in comparison to sham stimulation. Furthermore, we extend the original findings with the addition of a within-subjects comparison between stimulation to target region hMT+ and an active control, the forehead. We expect to find a significant contralateral stimulation effect for hMT+ only.

Introduction

Targeting a specific brain region with non-invasive brain stimulation (NIBS) clarifies that region's functional and causal role in subsequent behavioral change. By regulating behavior, based on application and type, NIBS has potential both as an experimental research method and in clinical applications. Transcranial random noise stimulation (tRNS) is a variety of transcranial electric stimulation (tES) in which an alternating current is passed between electrodes at random frequencies (Terney et al., 2008). tES has been shown to be more cost-effective, accessible, and well-tolerated than other NIBS, such as transcranial magnetic stimulation (TMS; Westwood, 2020). tRNS is a less commonly used method of tES in comparison to transcranial direct current stimulation (tDCS) and transcranial alternating current stimulation (tACS), however the application of tRNS is increasing rapidly. tRNS, unlike tDCS, has polarity independence and no uniform electrical field direction, meaning that it can target multiple brain regions simultaneously (van der Groen et al., 2022). High-frequency tRNS (hf-tRNS) is thought to enhance excitability and predominantly causes facilitatory effects on behavior, in some cases culminating in a performance increase of ~30% (Contò et al., 2021). tRNS has been demonstrated to enhance global motion direction discrimination (Ghin et al., 2018), fluid intelligence (Brem et al., 2018), numerosity (Cappelletti et al., 2013), arithmetic ability (Snowball et al., 2013), and spatial attention (Contò et al., 2021).

tRNS provides the research community with a method to demonstrate the causal impact of targeted brain regions on specific behaviors, with applications in the clinical community becoming increasingly evident. For example, Herpich et al. (2019) found that tRNS over the visual cortex improved visual motion perception in both healthy controls and cortically blind patients over the course of ten days. Further, they found that the effect persisted for at least six months without further stimulation, suggesting that long-term plastic change in sensory processing was responsible for the observed effect.

Along with evidence of successful neuromodulation, however, there are examples of a failure to replicate these effects. For example, Romanska et al. (2015) found that tRNS over lateral occipitotemporal cortices improved performance on a facial identity perception task. However, Willis et al. (2019) failed to replicate this effect. Changes in methodology, such as the use of a different face stimulus set or the application of a different stimulation intensity (1.5 mA as opposed to 1 mA) may have contributed to the lack of replicability. However, the variability in outcome highlights the critical importance of replication studies in highlighting the flexibility of the procedure, especially given the potential applications of tRNS.

Here, we propose to replicate the facilitatory effect of hf-tRNS over the human middle temporal complex (hMT+) on contralateral motion processing, initially demonstrated by Ghin et al. (2018). Specifically, they reported that hf-tRNS over the hMT+ and vertex (Cz) enhanced sensitivity to global motion in a dot array stimulus. The improvement in performance was specific to global motion processing in the visual field contralateral to stimulation. No such stimulation impact on contralateral global motion processing was found for anodal- or cathodal-tDCS, or sham stimulation.

The motivation to replicate the hf-tRNS effect in Ghin et al. (2018) is reinforced by the well-supported hypothesis that hMT+ is specific to contralateral global motion processing (Strong et al., 2017; Ajina et al., 2015; Braddick et al., 2001). Many NIBS studies have investigated the effects of stimulation over hMT+ on motion processing and have found reliable effects on neural activity and task performance (e.g. Antal et al., 2004; Antal et al., 2012; Campana et al., 2016; Pavan et al., 2019). Combined, these studies demonstrate that stimulation over hMT+ has consistent effects. For example, Antal et al. (2004) tested the impact of tDCS (anodal and cathodal) on hMT+, V1, and the motor cortex during a visuomotor coordination task and a

motion direction discrimination task. The authors found that only anodal-tDCS over hMT+ improved performance on these tasks. TMS over hMT+ has also been shown to modulate motion processing. For example, Laycock et al. (2007) found that single pulse TMS to hMT+ 158 ms after stimulus onset of a motion direction discrimination task disrupted task performance. Similarly, McKeefry et al. (2008) found that repetitive TMS over hMT+ and V3A caused deficits in speed discrimination, while TMS over adjacent areas and V1 did not. Finally, Campana, Maniglia, and Pavan (2013) found that repetitive TMS over hMT+ reduced the duration of dynamic and static motion after-effect.

Motion processing is predominantly lateralized, which enables the comparison of stimulation on the left and right visual fields as a within session control. A tDCS study found that cathodal-tDCS over left hMT+/V5 reduced a noisy signal while anodal-tDCS boosted a weak signal in the contralateral visual field only during a motion coherence task (Battaglini, Noventa, and Casco, 2017). Furthermore, repetitive TMS over left hMT+ impaired performance in a multiple object tracking task in the contralateral visual field only (Chakraborty et al., 2021). Due to strong theoretical support and evidence across NIBS techniques for the highly reliable effects of stimulation over hMT+, our study provides an ideal test for the replicability of hf-tRNS effects.

We propose to replicate and extend Ghin et al.'s (2018) findings by combining Experiments 1 and 2 in their paper. In Experiment 1, the authors employed a within-subjects design with three types of tES (cathodal-tDCS, anodal-tDCS, hf-tRNS) and sham stimulation. Each participant (n=16) underwent each type of stimulation over the course of four, non-consecutive sessions in which the active electrode was placed over left hMT+ and the reference electrode was placed over Cz. The authors applied stimulation during a motion direction task (i.e. online stimulation) which required participants to determine the overall direction of random dot kinematograms (RDK's), or fields of moving dots, during an eight alternative forced choice task. RDK's were

either shown to the left or right of a fixation dot in the middle of the screen. An adaptive maximum likelihood procedure (MLP) was used to determine the coherence threshold of the stimuli in each trial until the participants performed at 70% accuracy within 18 minutes (Grassi and Soranzo 2009). The authors found that only the hf-tRNS condition lowered the coherence threshold in the right visual field, contralateral to the active electrode placed over the left hMT+ (ipsilateral > contralateral = 10.51%). Anodal- and cathodal- tDCS had no impact on performance.

To verify that the effects of Experiment 1 were location-specific, Ghin et al. (2018) stimulated two control sites in Experiment 2. In the first control (n=12), the active electrodes were placed over Cz and the left forehead. This control examined if stimulation over Cz alone affected motion direction discrimination in Experiment 1. In the second control (n=12), the active electrodes were placed over Cz and the left primary visual cortex (V1) to determine if visual cortex stimulation was sufficient to improve motion direction discrimination. No significant effects on performance in the motion direction discrimination task were found in either control (Forehead: ipsilateral > contralateral = 1.17%; V1: ipsilateral > contralateral = 1.58%), apparently confirming the hypothesis that the observed effects of stimulation were specific to hMT+. However, the authors did not directly compare the hMT+ condition with the V1 or forehead control conditions.

Although we plan to replicate the contralateral impact of hf-tRNS over left hMT+ from Ghin et al., (2018), we will not perform an exact replication. We propose to include only a selection of the original conditions, and have introduced extra within-subject stimulation controls in our design. We will combine Experiments 1 and 2 from Ghin et al. (2018) to create a three condition within-subjects design: from Experiment 1, we will retain the hf-tRNS condition over left hMT+ to Cz, and sham condition over left hMT+ to Cz. Due to the lack of stimulation impact following

anodal- or cathodal-tDCS, we will not replicate these effects. In order to perform the direct comparison of hMT+ with another active hf-tRNS control site, from Experiment 2, we will adopt the hf-tRNS over the left forehead to Cz stimulation control rather than left V1 stimulation. Simulations of hMT+, forehead, and V1 stimulation (all in combination with Cz as the second electrode), demonstrated an overlap of stimulated posterior areas in the hMT+ and V1 simulations (see Appendix A). Due to the overlap of stimulated areas, we will not use hf-tRNS over V1 to Cz as an additional active control. Although we will maintain the original predetermined coordinate stimulation procedure of Ghin et al. (2018), we also propose to localize each participants' hMT+ using lateralized radial moving dots (Strong et al., 2017). We will use the localization to calculate the overlap between the predetermined coordinate stimulation and individual neural activity in response to lateralized motion processing. The measure of overlap between e-field flow and neural activity should correlate with stimulation effect on behavior. By maintaining the stimulation approach of Ghin et al. (2018), we ensure our replication is closer to the original study.

We have three main hypotheses: 1) We hypothesize that we will replicate the facilitatory effect of hf-tRNS to hMT+ on contralateral global motion processing in comparison to ipsilateral global motion processing. 2) We expect the facilitation for contralateral in comparison to ipsilateral motion processing will be larger for hMT+ in comparison to sham. 3) The facilitation for contralateral in comparison to ipsilateral motion processing will be larger for hMT+ in comparison to forehead stimulation.

We also will perform an exploratory analysis to examine if an increased overlap between the predetermined hMT+ targeted stimulation coordinates and neural response to processing lateralized motion predicts an increased impact of hMT+ targeted stimulation.

Methods

I. Participants

Forty-two participants will take part in the study, determined by the largest number of participants needed for the three effect sizes of interest using the data from Ghin et al. (2018). We performed three power analyses on the three comparisons of interest (See Appendix B). In each power analysis, the standard deviation is based on the Ghin et al. (2018) between-subjects design, providing a conservative estimate of variance for our within-subjects design. Based on these power analyses we predict 42 participants to be the maximum number of participants necessary for our within-subjects design. Participants will only be excluded from analysis if there is an equipment failure, or if the participant fails to attend all sessions. Participants will not be excluded due to outliers as the counterbalancing of the three stimulation sessions may lead to spurious outliers as a result of learning. The participants will be screened for normal or corrected-to-normal visual acuity and the ability to meet a 70% threshold during the constant thresholding procedure (see Appendix C). This study was approved by the Ethics Committee of the NIH. We will obtain written informed consent from each participant before taking part in the study, for which they will receive monetary compensation.

II. Apparatus

We will display stimuli on a ViewPixx monitor (21.25 x 12 inches) with a refresh rate of 60 Hz. Screen resolution is 1920 x 1080 pixels, with participants 25.65 inches from the screen. The minimum luminance of the screen is 0.51 cd/m^2, the maximum 84.35 cd/m^2, and the mean 42.58 cd/m^2. We will generate stimuli using Matlab with Psychtoolbox.

III. Stimuli

A. Random Dot Kinematograms (RDKs)

We will use random dot kinematograms (RDKs) presented in either the left or right visual field, the same stimuli as in Ghin et al. (2018) (Figure 1). Each RDK will consist of 150 white dots (0.12 deg diameter) and will be presented in a circular aperture (8 deg diameter; 3 dots/deg^2 density). The center of the aperture will be placed 12° to the left or right of fixation. Dots will drift at a speed of 13.3 deg/s, and will either last for 47 ms or reach the edge of the aperture before they will vanish and be replaced by new dots at a randomly selected position within the circular aperture. This will maintain dot density. Dots will appear asynchronously and belong to one of two categories: signal dots and noise dots. Signal dots will only move along one of the eight cardinal trajectories, while noise dots will appear at randomly selected locations within the aperture on each new frame. Further, dots will have an equal probability of being selected as a signal dot or noise dot to minimize motion streaks. Each RDK will last for 106 ms; the short duration of the stimuli is designed to prevent attentional tracking of motion direction and eye movements towards the RDK's. At the end of each RDK presentation, the participants will have three seconds to determine the overall direction of the moving dots in an eight-alternative forced choice task.

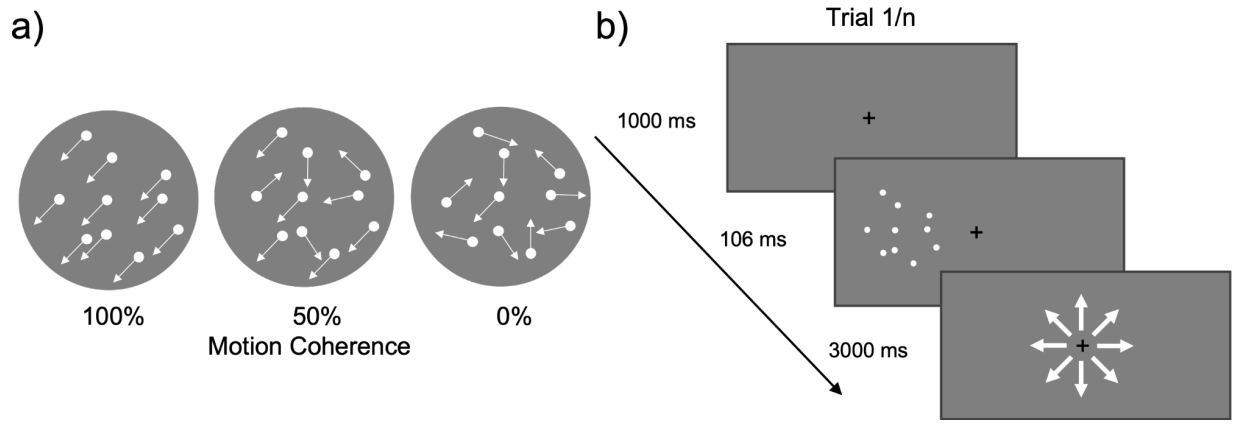

Figure 1. *Illustration of RDK's. a) RDKs with motion coherence of 100%, 50%, and 0%. B) A depiction of one trial of the motion discrimination task. RDKs will be randomly presented 12 dva to the left or right of fixation on each trial.*

B. Thresholding

In each visual field we will estimate the motion coherence threshold corresponding to 70% correct motion discrimination. Motion coherence will be reported as the percentage of dots moving in the same direction to enable successful motion discrimination. The motion coherence will be determined in each visual field using an interleaved adaptive maximum likelihood procedure (MLP; Grassi and Soranzo, 2009). MLP is a parametric adaptive thresholding procedure, which is less time consuming that non-parametric procedures. Adaptive means the percentage motion coherence for trial n+1 is selected based on the participants' response to the previous n trials. Adaptive procedures therefore maximize the number of trials presented close to threshold.

The threshold is estimated in five steps:

1. Collection of the n-th trial response
2. Fit the previous responses of n trials to hypothesized psychometric functions.
3. Selection of the psychometric function maximizing the likelihood of the previous n trials.
4. Using the selected psychometric function, estimate the percentage motion coherence to present for 70% performance accuracy.
5. Present the motion coherence percentage for the subsequent trial. The final estimated motion coherence percentage is the final coherence threshold.

Our psychometric functions

$$p(x) = \gamma + (1-\gamma \,/\, 1+exp\,(-\beta\,(x-\alpha)))$$

will have a fixed slope (β) of 1/2, a fixed baseline (γ) of 12.5% in accordance with chance level in an eight-alternative forced choice paradigm, and a target threshold (*p*) of 70%. The psychometric functions will only differ by midpoint (α), which will range across 150 values enabling presentation of 0-100% motion coherence at 70% accuracy. On each trial the MLP determines which of the hypothesized 150 psychometric functions best fit the data from the previous trials. The MLP code is adapted from Grassi and Soranzo (2009).

The coherence threshold will be estimated using MLPs across all 160 trials, presented over five blocks, during stimulation. Ghin et al. (2018) ran a MLP for each block and averaged across all five. In order to provide the MLPs with maximum trials, we will threshold across all five blocks combined.

C. Localizer stimuli

The left hMT+ will be identified for each participant using a fMRI localizer similar to the one described in Strong et al. (2017) (see Figure 2). Across two localizer runs, participants will view 32 blocks with apertures of moving or static dots presented 12° to either the left or right of fixation. Every four blocks, the participants will have a fixation block. Each block will be presented for 15 s. In the moving and static blocks, the 10° diameter aperture will contain 300 white dots (~0.2° diameter) presented on a black background. In the movement blocks, the dots will move at 7°/s radially alternating inwards and outwards. The participants will perform a task at fixation, pressing a button every time the fixation point turns pink.

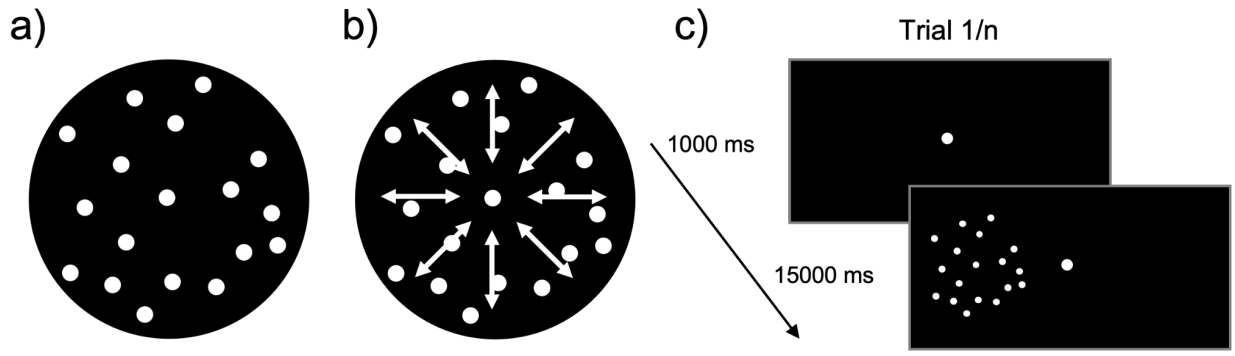

Figure 2. *Illustration of localizer stimuli.* A) *represents a static dot stimulus,* b) *represents a radial dot motion stimulus. C) A depiction of one block of the localizer. If F = fixation, MR = motion right of fixation, ML = motion left of fixation, SR = static right of fixation, SL = static left of fixation, the run presentation order will be as follows: Run 1: F, MR, SR, SL, ML, F, SR, ML, MR, SL, F, SL, MR, ML, SR, F, ML, SL, SR, MR, F. Run 2: F, ML, SL, SR, MR, F, SL, MR, ML, SR, F, SR, ML, MR, SL, F, MR, SR, SL, ML, F.*

IV. fMRI acquisition

We will use a 3.0T GE 750 MRI scanner in the fMRI facility in the Clinical Research Center on the National Institutes of Health campus in Bethesda, MD to collect the hMT+ localizer and MPRAGE anatomical scans. Gradient echo pulse sequences will be used with a 32-channel coil to measure blood oxygenation level-dependent (BOLD) signal during the functional localizer (TR = 2000 ms, TE = 39, Frequency FOV = 22.5 cm, 50 slices, 2.5 x 2.5 x 2.5 mm3, interleaved slice acquisition). A high-resolution T1-weighted anatomical will also be collected (208 slices, TR=7, TE= Min full, Frequency FOV = 25.6 cm, flip angle = 8°).

V. fMRI analysis and localization of the hMT+

The functional and anatomical MRI data will be preprocessed and analyzed using AFNI (Cox 1996). During preprocessing of the functional images, we will motion correct the data after removing the dummy scans from the analysis (n=3), allowing stabilization of the magnetic field. We will then align our functional data to each individual's anatomical and each volume of the

functional data set to the lowest motion volume. We will also blur each volume to 4mm fwhm and censor our data, removing runs where participants move more than 3mm. Multiple linear regression will then be applied, allowing for contrasts between moving and static blocks. hMT+ and other motion processing regions will be localized using a moving > static dots contrast in the contralateral visual field.

VI. Stimulation parameters and positioning

We will deliver stimulation using a battery-driven stimulator (NeuroConn DC STIMULATOR MC) and a pair of saline-soaked sponge electrodes. We will stimulate using hf-tRNS at 1.5 mA (crest to trough) alternating current with 0-offset and random frequencies at the capacity of our stimulator (range between 101 to 640 Hz). For the sham condition we will ramp up stimulation for 30 seconds before the task and stop stimulation during the task. Stimulation will last for a total of 18 minutes. Each electrode will have an area of 25 cm^2. We will keep the current density below safety limits (below 1 A/m^2). In the experimental and sham conditions, we will place one electrode over the left hMT+, and in the active control condition, over the forehead. The other electrode in all conditions will be placed over the vertex (Cz). Left hMT+ will be localized using predetermined coordinates, 3 cm dorsal of the inion and 4 cm leftward (Ghin et al., 2018). The vertex will be identified using Cz from the International 10-20 system, as in Ghin et al. (2018).

For the control stimulation, we will place one electrode over the left forehead, as described by Ghin et al. (2018). Additionally, using Brainsight to provide MNI coordinates for each participant's forehead stimulation location, we will simulate the stimulation e-fields with ROAST (Huang et al. 2019). Using these simulations, we will report which cortical regions may be impacted by the forehead stimulation, and we will report these regions and their potential influence over the task using data from Neurosynth.org (NeuroSynth, RRID:SCR_006798).

VII. Procedure

Our within-subjects design will require each participant to receive hf-tRNS targeted to the hMT+ and forehead, and sham stimulation to the hMT+ for a total of three non-consecutive sessions. We will counterbalance condition order to account for learning effects. Since we are interested in the effects of online stimulation, participants will perform the task during stimulation. Each participant will undergo a stimulation session consisting of 160 trials in each visual field split across five blocks. MLPs will be run on trials presented in each visual hemi-field (left and right). Over the course of one stimulation session, the coherence threshold for the left and right hemi-fields will be estimated from MLPs across all 160 trials.

We hypothesize that in the right visual field (contralateral to stimulation) the coherence threshold will be facilitated by hf-tRNS stimulation to the left hMT+, as was found by Ghin et al. (2018). We further hypothesize that neither stimulation to the forehead nor sham stimulation will modulate the coherence threshold. Participants will be blinded to the type of stimulation applied in each session.

Figure 3. *Experimental procedure according to visit. Visit 1 will consist of a hMT+ localizer in the fMRI (bottom left: localized left hMT+ (right motion > static)). For Visits 2-4, participants will perform the motion discrimination task under three different conditions. These are: the experimental condition, hMT+ stimulated with hf-tRNS, and two*

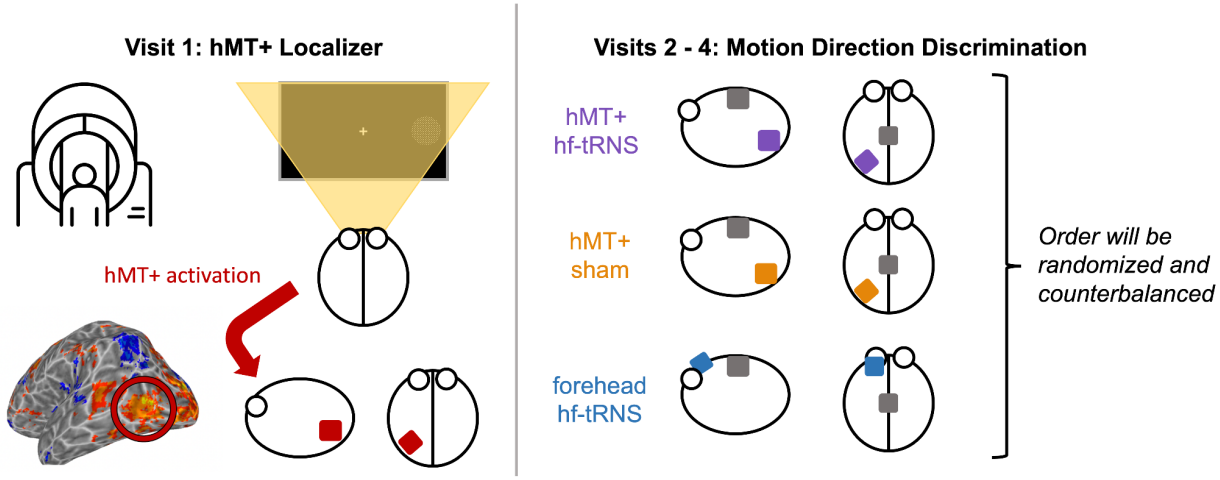

control conditions, hMT+ with sham stimulation and forehead stimulated by hf-tRNS. The order of Visits 2-4 will be randomized and counterbalanced.

VIII. Statistical analysis

We will perform three one-tailed paired sample *t*-tests to examine:

1. the decrease in motion coherence threshold to the visual field contralateral from stimulation in comparison to the visual field ipsilateral from stimulation following hf-tRNS to hMT+.
2. the difference between contralateral versus ipsilateral motion coherence thresholds following hMT+ targeted hf-tRNS versus the difference between contralateral versus ipsilateral motion coherence thresholds following sham hf-tRNS.
3. the difference between contralateral versus ipsilateral motion coherence thresholds following hMT+ targeted hf-tRNS versus the difference between contralateral versus ipsilateral motion coherence thresholds following forehead targeted hf-tRNS.

IX. Expected results

We expect to find a reduction in coherence threshold for hf-tRNS stimulation to the left hMT+ in the contralateral right visual field in comparison to ipsilateral left visual field. We also

expect the facilitation of contralateral in comparison to ipsilateral motion coherence threshold to be larger for hMT+ targeted hf-tRNS in comparison to hMT+ sham tRNS and for hMT+ targeted hf-tRNS in comparison to forehead targeted hf-tRNS.

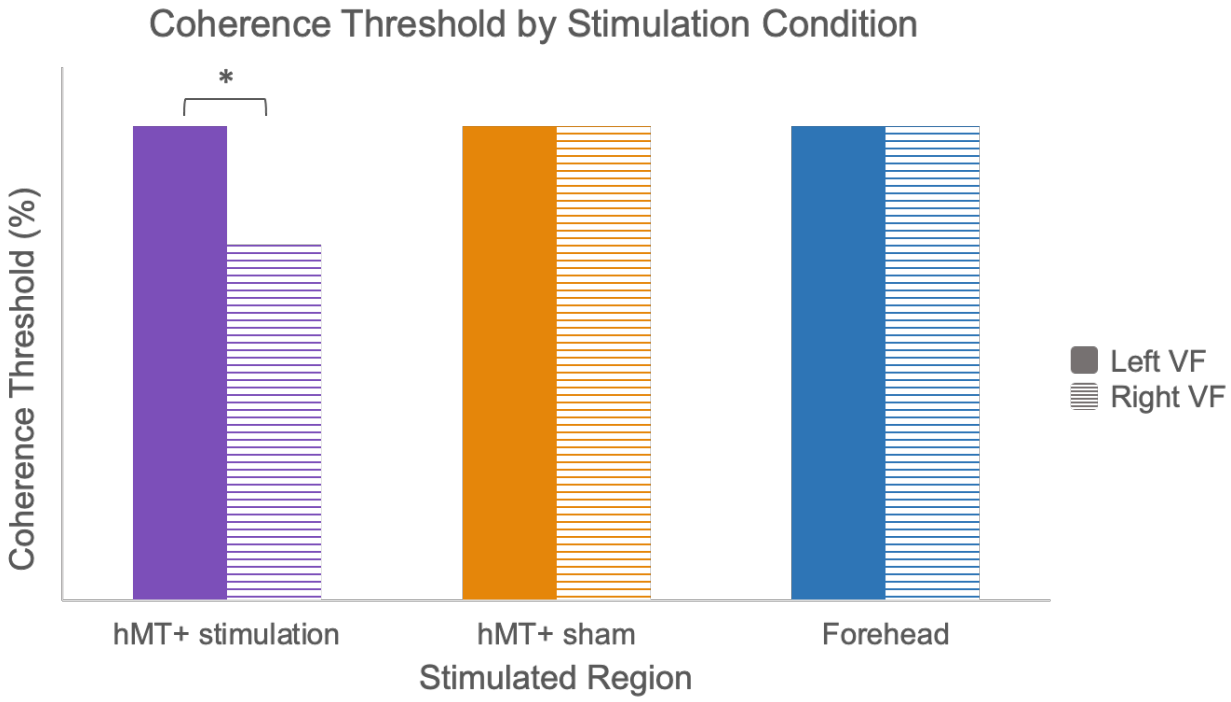

Figure 4. *Depiction of our expected results. Mean coherence thresholds for each stimulation condition, split by the left and right visual fields (VF). We expect to find a significant drop in coherence threshold for hMT+ stimulation in the right VF only.*

Table 1: Study Design Template

Question	Hypotheses	Sampling Plan & Test sensitivity rationale	Analysis plan	Rationale for deciding the sensitivity of the test for confirming or disconfirming the hypothesis	Interpretation given different outcomes	Theory that could be shown wrong by the outcomes
Question 1: Does stimulation targeted at left hMT+ facilitate motion processing in the contralateral visual field only?	**Hypotheses:** hf-tRNS targeted at left hMT+ will lower the percentage motion coherence threshold of the RDKs in the right visual field, contralateral from stimulation, in comparison to the ipsilateral left visual field. **Null hypotheses:** No difference in modulating right contralateral visual field motion coherence threshold in comparison to left ipsilateral motion coherence threshold following hf-tRNS targeted at left hMT+	42 participants will be included. We performed power analyses on our three contrasts of interest using data from Ghin et al., (2018) and determined our N from the smallest effect size. The contrast with the smallest effect size was that of **question 2**: the comparison of contralateral versus ipsilateral motion coherence thresholds following hMT+ targeted hf-tRNS with contralateral versus ipsilateral motion coherence thresholds following sham hf-tRNS.	We will perform a one-sided paired-samples *t*-test to assess whether the motion coherence threshold in the contralateral right visual field reduces significantly in comparison to the ipsilateral left visual field after hf-tRNS targeted at hMT+.	The effect size was estimated by performing three power analyses on our three comparisons of interest, We powered our study using the smallest effect size **(question 2**): The comparison of contralateral versus ipsilateral motion coherence thresholds following hMT+ targeted hf-tRNS with contralateral versus ipsilateral motion coherence thresholds following sham hf-tRNS estimated from Ghin et al. (2018) experiment 1. Specifically, the true mean: 10.51% difference in contralateral and ipsilateral motion coherence threshold	Hypothesis will be confirmed if there is a significant ($p<0.02$) decrease in motion coherence threshold of the right contralateral visual field in comparison to the left ipsilateral visual field following hf-tRNS targeted at hMT+. The null hypotheses will be accepted if there is no difference ($p>0.02$) on the contralateral motion coherence threshold in comparison to ipsilateral motion coherence following hf-tRNS targeted at hMT+.	If we find no evidence for our hypothesis, our study will demonstrate that the effect of hf-tRNS targeted at hMT+ on contralateral motion processing cannot be easily replicated. This may suggest the need for individualized targeting of stimulation site using functional imaging localizers, addressed in our exploratory analysis.

				following hf-tRNS targeted at hMT+. The null mean: 2.59% difference in contralateral and ipsilateral motion coherence threshold following sham tRNS targeted at hMT+. The standard deviation: 14.8% in the contralateral visual field following sham tRNS targeted at hMT+. Power=0.9 and type I error rate of 2%. Calculated n = 42.	
Question 2: Is hf-tRNS stimulation targeted at left hMT+ necessary to elicit the contralateral motion coherence change, or is the effect caused by the placebo effect of the application of the electrodes alone?	**Hypotheses:** A significantly larger difference in contralateral versus ipsilateral motion coherence threshold will be found following hf-tRNS targeted at hMT+ in comparison to sham tRNS targeted at hMT+ **Null hypotheses:** No significant difference will be found in contralateral versus ipsilateral motion coherence threshold	As above	We will perform a one-sided paired-samples *t*-test to assess whether the motion coherence threshold of contralateral versus ipsilateral visual fields is significantly larger following hf-tRNS targeted at hMT+ in comparison to sham.	As above	Hypothesis will be confirmed if there is a significantly ($p<0.02$) larger difference in motion coherence threshold for contralateral versus ipsilateral visual fields following hf-tRNS in comparison to sham tRNS to left hMT+ The null hypotheses will be accepted if there is no difference ($p>0.02$).	If we find no evidence for our hypothesis, our study will demonstrate that hf-tRNS targeted at hMT+ is not the sole cause of a decrease in contralateral motion coherence threshold. It is plausible the application of the electrodes alone are sufficient to cause an indistinguishable effect.

	following hf-tRNS targeted at hMT+ in comparison to sham tRNS targeted at hMT+					
Question 3: Is hf-tRNS stimulation targeted at left hMT+ necessary to elicit the contralateral motion coherence change, or can the effect be caused by hf-tRNS stimulation targeted at the forehead?	**Hypotheses:** A significantly larger difference in contralateral versus ipsilateral motion coherence threshold will be found following hf-tRNS targeted at hMT+ in comparison to hf-tRNS targeted at the forehead. **Null hypotheses:** No significant difference will be found in contralateral versus ipsilateral motion coherence threshold following hf-tRNS targeted at hMT+ in comparison to hf-tRNS targeted at the forehead.	As above	We will perform a one-sided paired-samples *t*-test to assess whether the motion coherence threshold of contralateral versus ipsilateral visual fields is significantly larger following hf-tRNS targeted at hMT+ in comparison to hf-tRNS targeted at the forehead.	As above	Hypothesis will be confirmed if there is a significantly ($p<0.02$) larger difference in motion coherence threshold for contralateral versus ipsilateral visual fields following hf-tRNS targeted at hMT+ in comparison to hf-tRNS targeted at the forehead. The null hypotheses will be accepted if there is no difference ($p>0.02$).	If we find no evidence for our hypothesis, our study will demonstrate that hf-tRNS targeted at hMT+ is not the sole cause of a decrease in contralateral motion coherence threshold. It is plausible stimulation to the control site, the forehead, is sufficient to cause an indistinguishable effect.

Appendix A: Simulations of stimulation montages

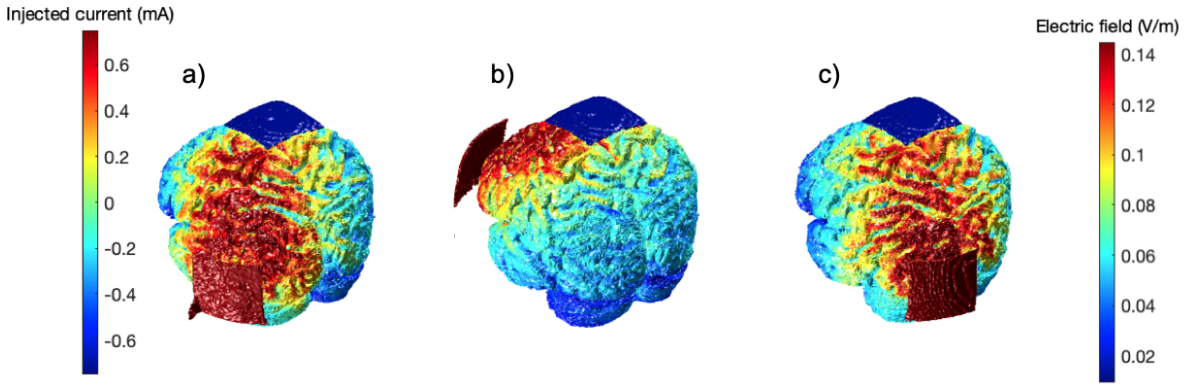

Appendix A, Figure 1: *Simulations of a) T5 (left hMT+) to Cz, b) Fp1 (left forehead) to Cz, c) O1 (left V1) to Cz using ROAST (Huang et al., 2019).*

Matlab Syntax:

Left hMT+ to Cz: roast('example/subject1.nii', {'T5',0.75,'Cz',-0.75}, 'electype', {'pad','pad'}, 'elecsize', {[50,50,3],[50,50,3]}, 'simulationTag', 'hMTsimulation')

Left forehead to Cz: roast('example/subject1.nii',{'Fp1',0.75,'Cz',-0.75}, 'electype',{'pad','pad'}, 'elecsize',{[50,50,3],[50,50,3]}, 'simulationTag', 'foreheadsimulation')

Left V1 to Cz: roast('example/subject1.nii',{'O1',0.75,'Cz',-0.75}, 'electype',{'pad','pad'}, 'elecsize',{[50,50,3],[50,50,3]}, 'simulationTag', 'V1simulation')

The active control of V1 to Cz as used by Ghin et al. (2018) is excluded from replication due to the overlap between the simulated electric field with the simulation of hMT+ to Cz. Overlap was quantified by analyzing the mutual information in the hMT+ and V1 simulations in comparison to the mutual information in the hMT+ and forehead simulations (Giangregorio, 2022). Where zero would denote complete independence between the simulations, and 2.5008 complete

dependence, hMT+ and V1 had a mutual information score of 1.2997, whereas hMT+ and the forehead had a mutual information score of 0.9485. Whilst some dependence is expected due to the same reference electrode position (Cz) in all montages, minimizing mutual information was preferable.

Appendix B: Power analyses

We performed three power analyses on our three comparisons of interest:

First, we examined contralateral versus ipsilateral motion coherence thresholds following hf-tRNS to hMT+. Specifically, we used a true mean of 28.75% related to the contralateral motion coherence threshold, null hypothesis mean of 39.26% related to the ipsilateral motion coherence threshold, and standard deviation of 17.56% from Experiment 1 of Ghin et al (2018). With a power of 0.9 and type I error rate of 2%, we calculated the need for 34 participants. Second, we examined the difference between contralateral versus ipsilateral motion coherence thresholds following hMT+ targeted hf-tRNS versus the difference between contralateral versus ipsilateral motion coherence thresholds following sham hf-tRNS. We used a true mean of 10.51% related to the difference in contralateral and ipsilateral motion coherence threshold for hMT+ targeted hf-tRNS, null hypothesis mean of 2.59% related to the difference in contralateral and ipsilateral motion coherence threshold for hMT+ targeted sham tRNS, and standard deviation of 14.8% from Experiment 1 of Ghin et al (2018). With a power of 0.9 and type I error rate of 2%, we calculated the need for 42 participants. Finally, we examined the difference between contralateral versus ipsilateral motion coherence thresholds following hMT+ hf-tRNS versus the difference between contralateral versus ipsilateral motion coherence thresholds following forehead targeted hf-tRNS. We used a true mean of 10.51% related to the difference in contralateral and ipsilateral motion coherence threshold for hMT+ targeted hf-tRNS, null hypothesis mean of 1.17% related to the difference in contralateral and ipsilateral motion

coherence threshold for forehead targeted hf-tRNS, and standard deviation of 8.44% from Experiment 1 of Ghin et al (2018). With a power of 0.9 and type I error rate of 2%, we calculated the need for 12 participants.

To maximally power our study for our three effect sizes of interest, we will collect 42 participants.

Appendix C: Screening participants for 70% motion discrimination

During piloting (see below), we were unable to establish a threshold at 70% correct on some participants due to poor performance. A threshold target of 70% is necessary for the maximum likelihood procedure thresholding to function. In order to replicate the original findings, rather than reduce the p-target, we will screen participants using a non-adaptive constant thresholding procedure.

Piloting the RDKs with non-adaptive constant thresholding

Using the same random dot kinematograms (RDKs) presented in motion discrimination task as described in the Stimuli section of the Method, we presented eight blocks of RDKs (n trials = 64) at a range of motion coherence levels from 25% to 100% in steps of 5%. This resulted in 32 trials per motion coherence level across all blocks. Using these data, we fit a psychometric function using a logit glm, and find the motion coherence at which participants were performing at 70% correct.

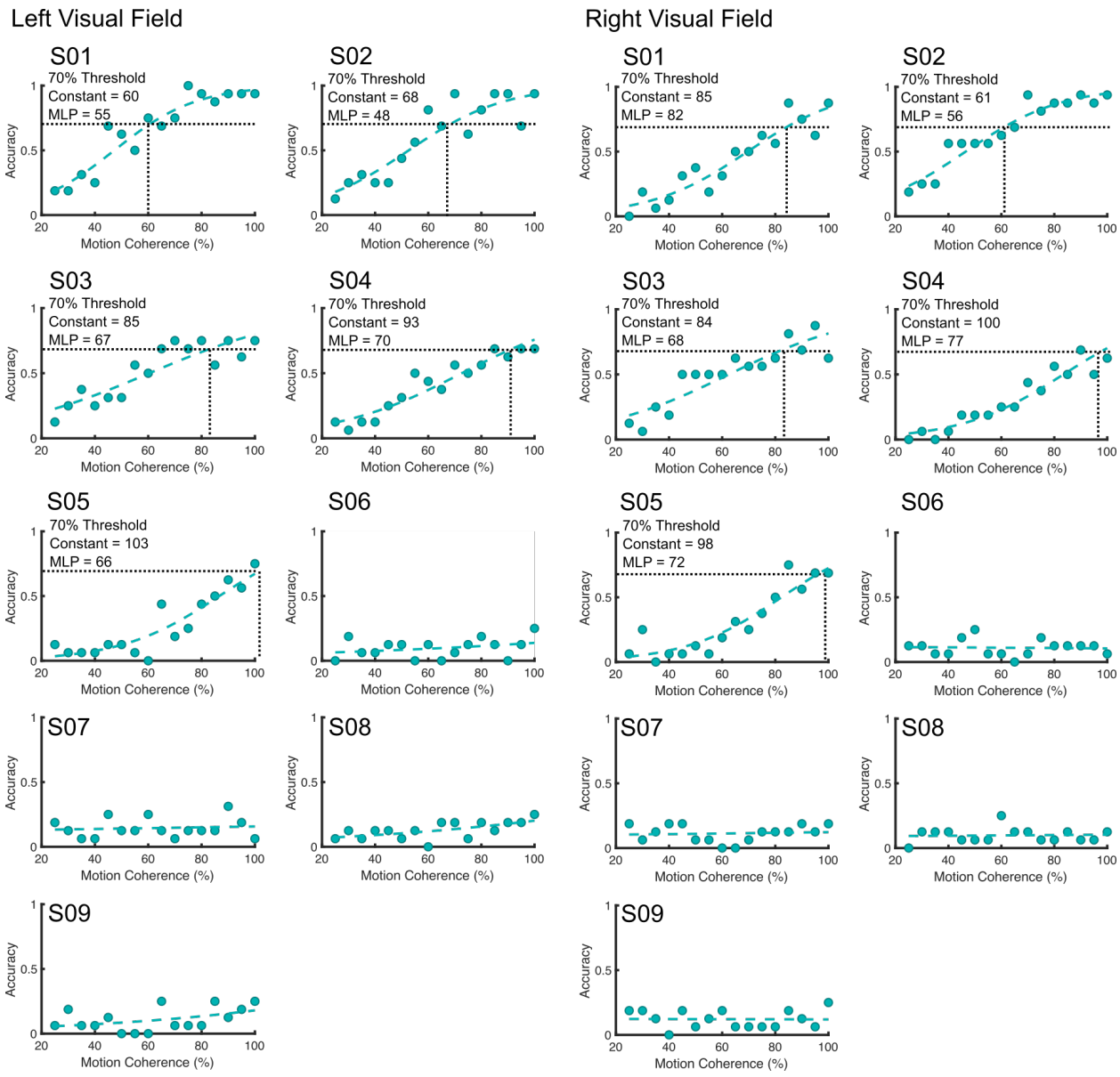

Appendix B, Figure 1: *Pilot data of nine participants in left and right visual fields. Data from the constant thresholding plotted with a psychometric function and MLP reported.*

We plot these functions for nine pilot participants in Appendix B, Figure 1. Five performed the motion discrimination task above 70% at one or more of the motion coherence levels, the other four performed below 70% at all motion coherence levels.

The five pilot participants able to perform the task above 70% correct returned for a second session using the MLP, and we found the MLP provided estimated thresholds lower than the constant thresholding performed in the first session, which may reflect a session effect of learning or increased sensitivity of the MLP approach.

References

Ajina, Sara, Christopher Kennard, Geraint Rees, and Holly Bridge. 2015. "Motion Area V5/MT+ Response to Global Motion in the Absence of V1 Resembles Early Visual Cortex." *Brain* 138 (1): 164–78. https://doi.org/10.1093/brain/awu328.

Antal, Andrea, Gyula Kovács, Leila Chaieb, Csaba Cziraki, Walter Paulus, and Mark W. Greenlee. 2012. "Cathodal Stimulation of Human MT+ Leads to Elevated FMRI Signal: A TDCS-FMRI Study." *Restorative Neurology and Neuroscience* 30 (3): 255–63. https://doi.org/10.3233/RNN-2012-110208.

Antal, Andrea, Michael A. Nitsche, Wolfgang Kruse, Tamás Z. Kincses, Klaus-Peter Hoffmann, and Walter Paulus. 2004. "Direct Current Stimulation over V5 Enhances Visuomotor Coordination by Improving Motion Perception in Humans." *Journal of Cognitive Neuroscience* 16 (4): 521–27. https://doi.org/10.1162/089892904323057263.

Battaglini, Luca, Stefano Noventa, and Clara Casco. 2017. "Anodal and Cathodal Electrical Stimulation over V5 Improves Motion Perception by Signal Enhancement and Noise Reduction." *Brain Stimulation* 10 (4): 773–79. https://doi.org/10.1016/j.brs.2017.04.128.

Braddick, Oliver J, Justin M D O'Brien, John Wattam-Bell, Janette Atkinson, Tom Hartley, and Robert Turner. 2001. "Brain Areas Sensitive to Coherent Visual Motion." *Perception* 30 (1): 61–72. https://doi.org/10.1068/p3048.

Brem, Anna-Katharine, Jessamy Norton-Ford Almquist, Karen Mansfield, Franziska Plessow, Francesco Sella, Emiliano Santarnecchi, Umut Orhan, et al. 2018. "Modulating Fluid Intelligence Performance through Combined Cognitive Training and Brain Stimulation." *Neuropsychologia* 118 (September): 107–14. https://doi.org/10.1016/j.neuropsychologia.2018.04.008.

Campana, Gianluca, Rebecca Camilleri, Beatrice Moret, Filippo Ghin, and Andrea Pavan. 2016. "Opposite Effects of High- and Low-Frequency Transcranial Random Noise Stimulation Probed with Visual Motion Adaptation." *Scientific Reports* 6 (1): 38919. https://doi.org/10.1038/srep38919.

Campana, Gianluca, Marcello Maniglia, and Andrea Pavan. 2013. "Common (and Multiple) Neural Substrates for Static and Dynamic Motion after-Effects: A RTMS Investigation." *Cortex* 49 (9): 2590–94. https://doi.org/10.1016/j.cortex.2013.07.001.

Cappelletti, M., E. Gessaroli, R. Hithersay, M. Mitolo, D. Didino, R. Kanai, R. Cohen Kadosh, and V. Walsh. 2013. "Transfer of Cognitive Training across Magnitude Dimensions Achieved with Concurrent Brain Stimulation of the Parietal Lobe." *Journal of Neuroscience* 33 (37): 14899–907. https://doi.org/10.1523/JNEUROSCI.1692-13.2013.

Chakraborty, Arijit, Tiffany T. Tran, Andrew E. Silva, Deborah Giaschi, and Benjamin Thompson. 2021. "Continuous Theta Burst TMS of Area MT+ Impairs Attentive Motion Tracking." *European Journal of Neuroscience* 54 (9): 7289–7300. https://doi.org/10.1111/ejn.15480.

Contò, Federica, Grace Edwards, Sarah Tyler, Danielle Parrott, Emily Grossman, and Lorella Battelli. 2021. “Attention Network Modulation via TRNS Correlates with Attention Gain.” Edited by Taraz Lee, Richard B Ivry, and Taraz Lee. *ELife* 10 (November): e63782. https://doi.org/10.7554/eLife.63782.

Cox, Robert W. 1996. “AFNI: Software for Analysis and Visualization of Functional Magnetic Resonance Neuroimages.” *Computers and Biomedical Research* 29 (3): 162–73. https://doi.org/10.1006/cbmr.1996.0014.

Ghin, Filippo, Andrea Pavan, Adriano Contillo, and George Mather. 2018. “The Effects of High-Frequency Transcranial Random Noise Stimulation (Hf-TRNS) on Global Motion Processing: An Equivalent Noise Approach.” *Brain Stimulation* 11 (6): 1263–75. https://doi.org/10.1016/j.brs.2018.07.048.

Grassi, Massimo, and Alessandro Soranzo. 2009. “MLP: A MATLAB Toolbox for Rapid and Reliable Auditory Threshold Estimation.” *Behavior Research Methods* 41 (1): 20–28. https://doi.org/10.3758/BRM.41.1.20.

Groen, Onno van der, Weronika Potok, Nicole Wenderoth, Grace Edwards, Jason B. Mattingley, and Dylan Edwards. 2022. “Using Noise for the Better: The Effects of Transcranial Random Noise Stimulation on the Brain and Behavior.” *Neuroscience & Biobehavioral Reviews* 138 (July): 104702. https://doi.org/10.1016/j.neubiorev.2022.104702.

Herpich, Florian, Michael D. Melnick, Sara Agosta, Krystel R. Huxlin, Duje Tadin, and Lorella Battelli. 2019. “Boosting Learning Efficacy with Noninvasive Brain Stimulation in Intact and Brain-Damaged Humans.” *The Journal of Neuroscience* 39 (28): 5551–61. https://doi.org/10.1523/JNEUROSCI.3248-18.2019.

Huang, Yu, Abhishek Datta, Marom Bikson, and Lucas C Parra. 2019. “Realistic Volumetric-Approach to Simulate Transcranial Electric Stimulation—ROAST— a Fully Automated Open-Source Pipeline.” *J. Neural Eng.*, 16.

Laycock, Robin, David P. Crewther, Paul B. Fitzgerald, and Sheila G. Crewther. 2007. “Evidence for Fast Signals and Later Processing in Human V1/V2 and V5/MT+: A TMS Study of Motion Perception.” *Journal of Neurophysiology* 98 (3): 1253–62. https://doi.org/10.1152/jn.00416.2007.

McKeefry, D. J., M. P. Burton, C. Vakrou, B. T. Barrett, and A. B. Morland. 2008. “Induced Deficits in Speed Perception by Transcranial Magnetic Stimulation of Human Cortical Areas V5/MT+ and V3A.” *Journal of Neuroscience* 28 (27): 6848–57. https://doi.org/10.1523/JNEUROSCI.1287-08.2008.

Pavan, Andrea, Filippo Ghin, Adriano Contillo, Chiara Milesi, Gianluca Campana, and George Mather. 2019. “Modulatory Mechanisms Underlying High-Frequency Transcranial Random Noise Stimulation (Hf-TRNS): A Combined Stochastic Resonance and Equivalent Noise Approach.” *Brain Stimulation* 12 (4): 967–77. https://doi.org/10.1016/j.brs.2019.02.018.

Romanska, Aleksandra, Constantin Rezlescu, Tirta Susilo, Bradley Duchaine, and Michael J. Banissy. 2015. “High-Frequency Transcranial Random Noise Stimulation Enhances Perception of Facial Identity.” *Cerebral Cortex* 25 (11): 4334–40. https://doi.org/10.1093/cercor/bhv016.

Snowball, Albert, Ilias Tachtsidis, Tudor Popescu, Jacqueline Thompson, Margarete Delazer, Laura Zamarian, Tingting Zhu, and Roi Cohen Kadosh. 2013. “Long-Term Enhancement of Brain Function and Cognition Using Cognitive Training and Brain Stimulation.” *Current Biology* 23 (11): 987–92. https://doi.org/10.1016/j.cub.2013.04.045.

Strong, Samantha L., Edward H. Silson, André D. Gouws, Antony B. Morland, and Declan J. McKeefry. 2017. “A Direct Demonstration of Functional Differences between Subdivisions of Human V5/MT+.” *Cerebral Cortex* 27 (1): 1–10. https://doi.org/10.1093/cercor/bhw362.

Terney, D., L. Chaieb, V. Moliadze, A. Antal, and W. Paulus. 2008. “Increasing Human Brain Excitability by Transcranial High-Frequency Random Noise Stimulation.” *Journal of Neuroscience* 28 (52): 14147–55. https://doi.org/10.1523/JNEUROSCI.4248-08.2008.

Westwood, Samuel James. 2020. “Investigating Cognitive and Therapeutic Effects of Transcranial Electric Stimulation (TES): A Short Guide for Reproducible and Transparent Research.” Preprint. PsyArXiv. https://doi.org/10.31234/osf.io/8qms2.

Willis, Megan L., Andrea I. Costantino, Michael. A. Nitsche, Romina Palermo, and Davide Rivolta. 2019. “Anodal TDCS and High-Frequency TRNS Targeting the Occipitotemporal Cortex Do Not Always Enhance Face Perception.” *Frontiers in Neuroscience* 13: 78. https://doi.org/10.3389/fnins.2019.00078.